Atmos. Chem. Phys. Discuss., 12, 31205–31245, 2012
www.atmos-chem-phys-discuss.net/12/31205/2012/
doi:10.5194/acpd-12-31205-2012

Atmospheric Chemistry and Physics Discussions

Impact of the marine atmospheric boundary layer on VSLS abundances in the eastern tropical and subtropical North Atlantic Ocean

S. Fuhlbrügge[1], K. Krüger[1], B. Quack[1], E. Atlas[2], H. Hepach[1], and F. Ziska[1]

[1]GEOMAR Helmholtz-Zentrum für Ozeanforschung Kiel, Kiel, Germany
[2]Rosenstiel School for Marine and Atmospheric Sciences, Miami, Florida

Received: 20 November 2012 – Accepted: 25 November 2012 – Published: 5 December 2012

Correspondence to: K. Krüger (kkrueger@geomar.de)

Published by Copernicus Publications on behalf of the European Geosciences Union.

Abstract

During the DRIVE ("Diurnal and Regional Variability of Halogen Emissions") ship campaign we investigated the variability of the halogenated very short-lived substances (VSLS) bromoform ($CHBr_3$), dibromomethane (CH_2Br_2) and methyl iodide (CH_3I) in the marine atmospheric boundary layer in the eastern tropical and subtropical North Atlantic Ocean during May/June 2010. Highest VSLS mixing ratios were found near the Mauritanian coast and close to Lisbon (Portugal). Air mass origins were calculated with 5-day backward trajectories starting at the surface and at the boundary layer top. We identified predominantly air masses from the open North Atlantic with some coastal influence in the Mauritanian upwelling area, due to the prevailing NW winds. Maximum VSLS mixing ratios above the Mauritanian upwelling were 8.92 ppt for bromoform, 3.14 ppt for dibromomethane and 3.29 ppt for methyl iodide, with an observed maximum diurnal variability up to 50 % for bromoform, 26 % for dibromomethane and 56 % for methyl iodide. A relationship was found between the marine atmospheric boundary layer (MABL) height and bromoform, dibromomethane and methyl iodide abundances. Lowest MABL heights above the Mauritanian upwelling area coincide with highest VSLS mixing ratios and vice versa above the open ocean. Significant high anti-correlations confirm this relationship for the whole cruise. We conclude that especially above oceanic upwelling systems MABL height variations are an important driver for VSLS mixing ratio variations and elevated atmospheric abundances and may explain the so far observed missing VSLS sources in this region.

1 Introduction

Natural halogenated very short-lived substances (VSLS) contribute significantly to the halogen contents of the troposphere and lower stratosphere (WMO, 2011). On-going environmental changes such as increases in seawater temperature and nutrient supply as well as decreasing pH are expected to influence VSLS production in the ocean.

ACPD
12, 31205–31245, 2012

Thus, the oceanic emissions of VSLS might change in the future and in connection with an altering efficiency of the atmospheric upward transport might lead to significant future changes of the halogen budget of the troposphere/lower stratosphere (Kloster et al., 2007; Pyle et al., 2007; Dessens et al., 2009; Schmittner et al., 2008; Montzka and Reimann, 2011). Within the group of brominated VSLSs bromoform ($CHBr_3$) and dibromomethane (CH_2Br_2) are the largest natural sources for bromine in the troposphere and stratosphere. In combination with iodine compounds (i.e. methyl iodide, CH_3I), tropospheric oxidation processes can be altered, including ozone depletion (Read et al., 2008). The VSLS have comparably short tropospheric lifetime (days to months); however, they can be rapidly transported by deep convection, especially in the tropics, to the upper troposphere and lower stratosphere and contribute to ozone depletion there (Warwick et al., 2006; WMO, 2007, 2011; Tegtmeier et al., 2012). Previous studies reported distinctive halocarbon emissions in tropical coastal and shelf water regions due to high biological productivity, i.e. by macro algae, seaweed and phytoplankton (Gschwend et al., 1985; Manley and Dastoor, 1988; Sturges et al., 1992; Moore and Tokarczyk, 1993; Carpenter and Liss, 2000; Quack et al., 2007). Elevated mixing ratios of the compounds have been found within the marine atmospheric boundary layer (MABL) around the Cape Verde Islands with a mean (range) for $CHBr_3$ of 8 (2.0–43.7) ppt, CH_2Br_2 of 2 (0.7–8.8) ppt and CH_3I of 3 (0.5–31.4) ppt (O'Brien et al., 2009) and in the area of the Mauritanian upwelling with a mean (range) of $CHBr_3$ around 6 (3–12) ppt (Carpenter et al., 2007; Quack et al., 2007) and CH_2Br_2 with 2.4 (1.75–3.44) ppt by Quack et al. (2007). These mean mixing ratios from the tropical Atlantic Ocean coincide well with other tropical oceanic areas (e.g. Atlas et al., 1993; Butler et al., 2007). Quack et al. (2004) suggested regionally enhanced biogenic production in the water column of the Mauritanian upwelling and a high sea-to-air flux of VSLS to be responsible for elevated tropospheric VSLS mixing ratios in this region. However, Carpenter et al. (2007) and Quack et al. (2007) both pointed out that the marine boundary layer height, besides additional potential coastal sources, may affect the tropospheric VSLS mixing ratios as well. The theory of warm offshore air flowing over cool water

ACPD
12, 31205–31245, 2012

and creating a stable internal boundary layer as drafted by Garratt (1990), applies well in the area of the cold Mauritanian upwelling. Here the sea surface roughness and near surface turbulence downsize each other over the water, while the flow leads to a collapse of turbulence and a very stable stratification of the lowermost atmosphere, as was observed by Vickers et al. (2001) at the coast of the United States and modelled by Skyllingstad et al. (2005).

In this study, we present first results from the DRIVE ("Diurnal and Regional Variability of Halogen Emissions") ship campaign during May/June 2010, comprising high resolution meteorological and VSLS measurements. We investigate the meteorological constraints on the VSLS abundances and whether the cold waters upwelled along the Mauritanian coast have a verifiable influence on the atmospheric boundary layer height and therefore on the mixing of air within the lowermost troposphere. While, in this study we focus on the atmospheric VSLS abundances during die DRIVE ship campaign, the accompanying study by Hepach et al. (2012) investigates the VSLS sources in the ocean and the drivers of the sea-to-air fluxes in more detail.

This paper begins with a short overview of the meteorological conditions during the DRIVE cruise, followed by a data and method description (Sect. 2). In Sect. 3 we present results from the meteorological and VSLS measurements and the influence of meteorology and MABL height on the VSLS mixing ratios and emissions. Finally, the summary is given in Sect. 4

2 Data and methods

Cruise overview

During May/June 2010 the DRIVE (P399/2-3) campaign, examined the formation and emission of halocarbons and reactive inorganic halogen compounds in the eastern tropical and subtropical North Atlantic Ocean (Bange et al., 2011) as part of the SOPRAN (Surface Ocean Processes in the Anthropocene: www.sopran.pangaea.de)

ACPD
12, 31205–31245, 2012

project. The main objectives were the investigation of the diurnal and regional variability of marine short-lived substances, as well as the mutual interaction between ocean and atmosphere.

The ship expedition was carried out on board of the German research vessel (R/V) Poseidon. The cruise itself was split into two legs: P399/2 (31 May–17 June 2010) and the transit P399/3 (19–24 June 2010). For diurnal observations, six 24 h stations with hourly VSLS measurements were performed during leg P399/2. Positions and times of the 24 h stations are given in Table 1. The location of the 24 h stations were chosen to cover the nutrient-rich regions in the coastal upwelling near the Mauritanian coast as well the nutrient-poor regions near the Cape Verde Islands. In addition 21 atmospheric VSLS samples were taken during the return from the last station in the Mauritanian upwelling to Las Palmas (Gran Canaria). During the transit leg P399/3 from Las Palmas to Vigo, Spain, additional 20 atmospheric air samples were taken.

Meteorology and MABL height

Meteorological data have been collected by the automatic on-board weather station of the German Weather Service (DWD): Air and water temperatures, wind speed and direction, humidity and air pressure were recorded once per second and are averaged to 10 min means for our analysis. GRAW DFM-06 radiosondes (http://www.graw.de) were launched from the working deck of R/V Poseidon at about 3 m a.s.l. during the cruise to profile the atmospheric composition of air temperature (resolution: 0.1 °C, accuracy: <0.2 °C), relative humidity (resolution: 1 %, accuracy: <5 %), and wind (wind speed accuracy: <0.2 m s^{-1}, accuracy horizontal position: < 5 m s^{-1}) (http://www.gematronik.com/fileadmin/media/pdf/GRAW-Brochure_V01.30_en.pdf) from the sea level up to the middle stratosphere (~30 km altitude). During the 24 h stations, the launch frequency was increased from one radiosonde per day at 12:00 UTC to 04:00 per day at 00:00, 06:00, 12:00 and 18:00 UTC amounting to 41 launches for the whole cruise.

ACPD
12, 31205–31245, 2012

The atmospheric boundary layer height is determined after the approaches summarized by Seibert et al. (2000). These methods include practical and theoretical determinations from radiosoundings. The vertical extension of the boundary layer is in general limited aloft by a temperature inversion or a stable layer, or by a significant reduction in air moisture. Two general types of boundary layers exist, the convective boundary layer (CBL), whose stable layer is found between the lower 100 m of the atmosphere and about 3 km height, and the stable boundary layer (SBL), characterized by a surface inversion. In case of a CBL, it is recommended to take the height of the base of the inversion, increased by half of the inversion layer depth (Stull, 1988). For a SBL we assume the absence of turbulence and vertical mixing (Garratt, 1990) and further declare the boundary layer to stay close to the surface (~0 m). According to this, we subjectively determined the height of the boundary layer in our study from the temperature and humidity profiles, and additionally from the bulk Richardson number by the following equation (Troen and Mahrt, 1986; Vogelezang and Holtslag, 1996):

$$Ri_{\mathrm{B}} = \frac{gz(\theta_z - \theta_s)}{\theta_s(u^2 - v^2)} \quad (1)$$

The quantities g and z are the gravitation acceleration and the geometric height. θ_z and θ_s are the virtual potential temperature at the height z and at the surface, and u and v are the zonal and meridional wind components. The virtual potential temperature can be seen as stability criterion for the atmosphere, considering the current air moisture. It is constant with height for neutral conditions, increases for stable conditions and decreases if the air is statically labil. To identify the boundary layer height theoretically, a fixed critical bulk Richardson number of $Ri_{\mathrm{c}} = 0.25$ is chosen as a threshold, following Sorensen (1998), where $Ri_{\mathrm{B}} \geq Ri_{\mathrm{c}}$. Due to missing wind data in the lowermost atmosphere during a number of radiosonde launches (failure of GPS sensor), we were not always able to determine Ri_{B} for the lower meters of the boundary layer. Therefore we use the subjectively determined boundary layer height for our investigations and calculate Ri_{B} to confirm our determined MABL height.

ACPD
12, 31205–31245, 2012

Air mass origin

For the analysis of the air mass origin, HySplit trajectories (http://ready.arl.noaa.gov/HYSPLIT.php), based on NCEP/NCAR Reanalysis 1 (NNR), are calculated online. The NNR is a first-generation reanalysis from 1948 to real time and has a horizontal resolution of 208 km (T62) and a vertical resolution of 28 levels (L28) with a model top at about 3 hPa. The data are globally distributed on a 2.5° latitude × 2.5° longitude Gaussian grid with a total of 144 × 73 grid points (Kalnay et al., 1996; Kistler et al., 2001).

VSLS measurements

187 air samples were taken on the monkey deck of R/V Poseidon, about 10 m height above sea level. The air was pressurized up to 2 standard atmospheres in pre-cleaned stainless steel canisters with each a volume of 2.6 l. The air samples were analysed according to the method by Schauffler et al. (1999) after the cruise at the Rosenstiel School for Marine and Atmospheric Sciences (RSMAS, Miami–Florida).

Our study concentrates on the atmospheric abundances of three VSLS: methyl iodide with a lifetime of ∼4 days (Solomon et al., 1994), bromoform of ∼26 days (Ko et al., 2003) and dibromomethane of ∼120 days (Ko et al., 2003). The precision for these VSLS measurements is estimated to be on the order of 5 %.

Sea to air flux calculations

Sea to air fluxes (F) of methyl iodide, dibromomethane and bromoform were calculated by Hepach et al. (2012) with the air-sea gas transfer coefficient k_w and the air-sea concentration gradient Δc:

$$F = k_w \cdot \Delta c. \quad (2)$$

ACPD
12, 31205–31245, 2012

The parameterization of Nightingale et al. (2000), based on instantaneous wind speeds (10 min averages) and temperature-dependent Schmidt numbers according to Quack and Wallace (2003), was applied to determine k_w. Δc was calculated from all simultaneous water and air measurements. For further details of oceanic concentrations and fluxes of the three VSLS see Hepach et al. (2012).

3 Results

3.1 Meteorology

The cruise was mainly exposed to moderate weather conditions. Contrary to the climatological wind direction of north-easterly trade winds in the subtropics and Westerlies north of 30° N during May/June, the mean absolute wind direction was NNW (Fig. 1) with a mean direction of 349° during leg 2 and 344° during leg 3. This caused a predominant influence of air masses with marine background conditions coming from the open North Atlantic Ocean. The mean wind speed during the whole cruise was moderate to fresh for both legs, with $7.4\,m\,s^{-1} \pm 2.9\,m\,s^{-1}$ during leg 2 and $9.3\,m\,s^{-1} \pm 1.6$ during leg 3. Higher average wind speeds were observed from 6 to 14 June 2010 between 16° N and 20° N, nearly matching the mean wind speed of leg 3. The total air pressure difference of 13.4 hPa also reflects the moderate and steady weather conditions during the whole cruise. A minimum of 1007.6 hPa was reached on 11 June 2010 close to the Mauritanian coast, when the ship approached the boundary of a low pressure system, originated at the border of Senegal and Mauritania (Fig. 2). The maximum air pressure of 1021 hPa was reached at the beginning of leg 3 on 19 June 2010 close to the Canary Islands. In addition diurnal variations up to 4 hPa, which are typical for the tropics (Krüger and Quack, 2012), due to atmospheric tides were observed. The 10 min average time series of the measured surface air – (T_{SAT}) and sea surface temperatures (T_{SST}) and the according regional difference ΔT (T_{SAT}–T_{SST}) are shown in Fig. 3. The temperature difference is related to the heat flux between atmosphere and ocean. A

ACPD
12, 31205–31245, 2012

positive ΔT reflects higher surface air temperatures than sea surface temperatures, leading to a heat flux from the atmosphere into the ocean and indicates suppressing of convection, turbulence and therefore mixing within the boundary layer. On the opposite, mixing is enhanced if the heat flux gets negative, due to higher sea surface temperatures than surface air temperatures. As the ship cruise started to the south, the air and water temperatures increase until the maximum air temperature of 25.8 °C is recorded right after the stop at Mindelo (Cape Verde Islands), followed by a decrease of T_{SAT} and T_{SST} towards the 3rd station. After this 24 h station and close to the Mauritanian coast, air and water temperatures rise again. On 11 June 2010, right after the 4th 24 h station, the ship reached the Mauritanian upwelling at 18.75° N, 16.5° W. This is distinguishable from the abrupt decrease in the water temperature and connected to an increase of the heat flux from the atmosphere to the ocean. After a time lag of about one day, the air temperature also drops, until T_{SAT} and T_{SST} stabilize between 18 °C and 20 °C (station 5). On 14 June 2010, after the ship has left the last 24 h station, the water temperature increases to about 23.5 °C. This increase coincides with a wind speed maximum of about 16 m s^{-1} from the north. Warmer water masses from outside the Mauritanian upwelling may be transported towards the ship at this time or the research vessel actually left the small upwelling belt, until the water temperature dropped again to about 18 °C. On 15 June 2010 the ship left the Mauritanian upwelling, indicated by increasing air and water temperatures until both decreased again with increasing latitude. A sudden decrease of the water temperature is also observed from 23 to 24 June 2010, as the ship enters the Iberian upwelling (Relvas and Barton, 2002). During this time the heat flux becomes and stays negative (Fig. 3), supporting convective activity and mixing, until the end of the cruise.

3.1.1 Marine atmospheric boundary layer

In the following, we use the radiosondes measurements to analyse the state of the lower atmosphere. Profiles of underway air temperature along the cruise track are shown in Fig. 4. Lowest temperatures of −80 °C are observed between 2 June and 15

ACPD
12, 31205–31245, 2012

June 2010 at 17 km height, indicating tropical air masses south of 25° N during leg 2. Two different tropopause definitions are used to identify the transition between tropical and extra-tropical air masses. The cold point tropopause (CPT) is defined as the minimum temperature in the vertical temperature profile and is commonly used for the tropics (Highwood and Hoskins, 1998). For the tropopause definition in the extratropics the lapse rate tropopause (LRT) criteria is calculated, which is defined as the lowest level at which the lapse rate decreases to 2 K km^{-1} or less. In addition the lapse rate is requested not to exceed 2 K km^{-1} within 2 km above this level (WMO, 1957). During leg 2, the heights of the CPT and LRT are detected between 16 and 17 km altitude with only slight difference between them and short-time variations. With regard to the different shapes and heights of the tropical and extra-tropical tropopauses, a change of the atmospheric regime is reflected by the decrease of the LRT height to 15 km in contrast to the CPT height after 15 June 2010 at the end of leg 2, as the ship enters the extra-tropics. The air temperature profiles of the radiosondes also reveal "trade inversions" between 1 and 2 km height from the beginning of the cruise until 4 June and from 16 June 2010 until the end of the cruise. These temperature inversions are typically found over eastern boundaries of tropical oceans (Neiburger et al., 1961). Beginning on June 4 2010, the temperature inversions descend in height, until they migrate, due to cold upwelling deep water (Fig. 3) in the Mauritanian upwelling, to intense surface inversions. The neutral and stable stratification of the lower 3 km of the troposphere and therefore the upper limit of the boundary layer during the cruise is shown by the virtual potential temperature gradient in Fig. 5. The subjectively and theoretically derived MABL heights (see Sect. 2) show a good compliance to each other. Differences between both MABL heights are found above the Mauritanian upwelling, due to missing near-surface winds for the calculation of the bulk Richardson-number, but also at the end of leg 2 and the beginning of leg 3, which may be caused by our fixed Ri_c, we took for convenience.

Except for the area at and south of the upwelling from 11 June to 14 June 2010, where we observed a SBL, the cruise was predominantly characterized by CBLs. The boundary layer height shows no distinct short time or diurnal variations, considering

ACPD
12, 31205–31245, 2012

the launch frequency of one radiosonde at 12:00 UTC each day and four radiosondes (6-hourly) per 24 h stations. The overall pattern bares boundary layer heights from the surface up to 400 m at the upwelling area and about 400–2000 m above the open ocean. These numbers coincide with the heights derived from trajectory models from previous studies along the Mauritanian coast (Carpenter et al., 2007; Quack et al., 2007). A strong temporal variation of the MABL height is found around the Canary Islands. While the boundary layer height is about 150 m on 31 May, it increases to 1.8 km in the same area at the southwest coast of Gran Canaria on 17 June 2010. During leg 3 the top of the boundary layer decreases from 1.4 km north of the Canary Islands to about 500 m near the coast of the Iberian Peninsula. The height of the MABL is also well reflected in the profiles of the relative humidity during the whole cruise as shown in Fig. 6 for the troposphere up to 10 km height. The measurements show the presence of clouds within 2 and 7 km height from 3 June to 14 June 2010, which are, according to the indifferent or even negative heat flux (Fig. 3), not due to local convection but rather due to advection of the clouds from southeast (not shown here). The increase of the surface / lower most troposphere humidity between 15 June and 22 June 2010 (Fig. 6) matches the observed elevation of the negative heat flux (Fig. 3). The height of the atmospheric boundary layer, determined from temperature observations, agrees very well with the surface maximum of relative humidity, underlining the good quality of relative humidity measurements from the GRAW sonde in this layer (Fig. 6). The vertical mixing within the MABL seems to be quite well reflected by the relative humidity observations. Especially, the small extension of enhanced relative humidity above the surface of the Mauritanian upwelling from 11–12 June 2010 further nails the assumption of reduced vertical mixing (turbulence) in this area due to the positive heat flux, leading to a very stable and narrow MABL.

3.2 Atmospheric VSLS variability

The diurnal and regional variations of the halogenated trace gas abundances in the MABL have been observed with hourly measurements at six 24 h stations near the

ACPD
12, 31205–31245, 2012

Cape Verde Islands and in the Mauritanian upwelling. According to the regional distribution of the diurnal stations (Fig. 1), the first two stations (S1, S2) can be combined to an open ocean cluster. The following 4 diurnal stations are furthermore declared as coastal stations (S3–S6), since they show similar characteristics in the surface water (for details see Hepach et al., 2012). In addition, six-hourly underway trace gas measurements have been taken from the last diurnal station on 14 June 2010 to Las Palmas and during leg 3 (19 June–23 June 2010). In between, along the coast of Gran Canaria (17 June 2010), the frequency was increased to hourly measurements. An increase of atmospheric mixing ratios from the Cape Verde Islands to the Mauritanian upwelling area is found for all three trace gases: bromoform (Fig. 7), dibromomethane (Fig. 8) and methyl iodide (Fig. 9). Within the open ocean cluster, the mixing ratios ranged between 0.48–9.9 ppt with a mean of 1.74 ppt for $CHBr_3$, 0.91–1.59 ppt and a mean of 1.28 ppt for CH_2Br_2 and 0.63–1.32 ppt with a mean of 0.93 ppt for CH_3I. With a mean $CH_2Br_2/CHBr_3$ ratio of 1.21 (Table 2) typical open ocean air masses were observed (Quack et al., 2004; Butler et al., 2007). At the third 24 h station, the bromocarbons show an increase to 4.22–6.12 ppt for $CHBr_3$ and 1.96–2.42 ppt for CH_2Br_2. In contrast, CH_3I reveals similar mixing ratios as at the open ocean stations. A mean $CH_2Br_2/CHBr_3$ ratio of 0.41 now indicates fresher oceanic sources. Slightly increased atmospheric mixing ratios of $CHBr_3$ with 4.21–6.58 ppt and of CH_2Br_2 with 2.04–2.87 ppt, and $CH_2Br_2/CHBr_3$ ratio of 0.46 are found at the 4th 24 h station. For the first time, the CH_3I mixing ratios show intense variations of 1.11–2.68 ppt at this coastal station. In addition, a diurnal pattern is striking for all three VSLS at this station (S4, Fig. 7). They show a slight decrease from 12:00 UTC to 00:00 UTC (UTC is equal to local time) followed by an increase from 06:00 UTC to 09:00 UTC on the following day, which hints towards an increased source coinciding with the sun rise at about 06:30 UTC. The highest atmospheric mixing ratios for all three VSLS during leg 2 were observed during the 5th station at 19° N and 16.5° W. All measurements show the most pronounced variations within one day at this station with mean mixing ratios of 3.57 ppt ($CHBr_3$), 0.67 ppt (CH_2Br_2) and 1.85 ppt (CH_3I). $CHBr_3$ gains maximum mixing ratios of 8.92 ppt, CH_2Br_2

ACPD
12, 31205–31245, 2012

of 3.14 ppt and CH_3I of 3.29 ppt. With regard to the hourly measurements of methyl iodide during station 5, the minimum at 05:00 UTC seems to be an outlier due to the high variation of more than 1 ppt within two h. Although, this station has the lowest $CH_2Br_2/CHBr_3$ ratio of 0.40 during leg 2, this value is two to three times higher than previously reported ratios of 0.1–0.25 for coastal source regions in the North Atlantic Ocean and the Northwest of Tasmania by (Carpenter et al., 2003) and tropical islands and the open Pacific Ocean by (Yokouchi et al., 2005). While the ship moved away from the Mauritanian coast, southwest of the Banc d'Arguin National Park, the last coastal station (S6) shows an increase of the $CH_2Br_2/CHBr_3$ ratio to 0.44 and a decrease of the trace gas mixing ratios down to a mean of 4.85 ppt (min-max: 4.07–6.01 ppt) for bromoform, 2.11 ppt (1.87–2.34 ppt) for dibromomethane and 1.28 ppt (1.07– 2.71 ppt) for methyl iodide. At station 6, an outlier seems to occur again in the methyl iodide measurements, in this case a maximum at 15:00 UTC, with regard to the remaining hourly measurements at this station. A further decrease of the atmospheric abundances is observed from this last 24 h station up to 22° N. Following from there back to the Canary Islands, the mixing ratios remain nearly constant, except for methyl iodide that shows a maximum of 2 ppt southwest of Gran Canaria. At the coast of Gran Canaria minor variations within the mixing ratios occur for all three VSLS. The mean mixing ratios observed at this Canarian coast of 2.29 ppt $CHBr_3$, 1.38 ppt CH_2Br_2 and 1.14 ppt CH_3I, however, are in agreement with the abundances detected over the open ocean stations.

During leg 3 the mixing ratios of the three trace gases are in the range of typical open ocean abundances. An increase of the brominated halocarbons is observed from 35° N towards the Portuguese coast. While dibromomethane only has a top mixing ratio of 2.70 ppt during this leg, bromoform reaches the highest mixing ratio observed during the whole DRIVE cruise close to Lisbon (Portugal), leading to a ratio of both compounds of 0.27. The comparatively high atmospheric abundances and the resulting low ratio indicate a close-by, fresh source in this area. Raimund et al. (2011) related the increased abundances of halogenated trace gases in the Iberian Upwelling system

ACPD
12, 31205–31245, 2012

to strong intertidal coastal sources and advection of halocarbon enriched coastal upwelling, but also anthropogenic sources as the river outflow are likely (Quack and Wallace, 2003).

3.2.1 Air mass origin

Investigating the air mass history is a good way to reveal potential source regions. Figure 10 shows HySplit trajectories, started at the ground and at the top of the boundary layer. A band of trajectories were run backwards for 120 h (5 days), starting each day of the cruise at 12:00 UTC. The upper plots show the horizontal and the lower plots the vertical distribution of the trajectories. Surface (ST) and boundary layer height trajectories (BLT) indicate primarily northerly origin of air masses during the cruise. At the beginning of leg 2 the air masses mainly arrive from the Azores. While the HySplit model projects that the STs do not extend 100 m altitude, the BLTs arise from about 3 km height with little Moroccan influence. A high pressure system, located between the Azores and the coast of Portugal, deflects the air masses up to 40° N–50° N close to the coast of Portugal and redirects, in combination with the trade winds, the air southwards to the ship. From 6 June to 17 June 2010 the light blue, yellow and orange trajectories show a more varying origin, between 30° N and 60° N. Most of the STs descend from heights up to 300 m to the surface 1–2 days before hitting the ship. This air mass descend is typical for a high pressure system. Reaching the ground, the surface inversions, as described in Sect. 3.1.1, prevent the air masses from ascending. The resulting stable, isolated and very low boundary layer leads to similar origins of offshore STs and BLTs. In the area of the Mauritanian upwelling, from 10–15 June 2010, the trajectories also pass the West coast of Mauritania and the western part of West Sahara within the last 24 h, however the air is predominantly approaching from the North Atlantic Ocean between 45° N–60° N and west of Great Britain. These origins have also been observed in previous measurement campaigns in this region of the eastern tropical North Atlantic Ocean (Quack et al., 2007) and (Carpenter et al., 2010). In comparison, the BLTs are spatially more widespread over the North Atlantic

ACPD
12, 31205–31245, 2012

Ocean, indicating the higher wind speed in the free troposphere. At leg 3 the STs and BLTs have a mid to polar latitude origin (30° N to 80° N), however continental influences from northern Europe are dominating for the BLTs, east of the prime meridian.

3.3 Meteorological constraints on VSLS variability

To distinguish meteorological constraints on the VSLS abundances we correlate meteorological parameters with bromoform, dibromomethane and methyl iodide (Table 3). In the following we highlight the significant correlations. We find a weak positive but significant correlation between the trace gas abundances and the wind speed for the open ocean and for the whole cruise. In contrast, the wind direction reveals an overall negative correlation of −0.5 for the brominated halocarbons and −0.3 for methyl iodide. This means increased VSLS abundances generally coincide with westerly winds and reduced abundances coincide with easterly winds during the whole cruise. To evaluate land-sea breeze constraints on the trace gas abundances, we take a look to stations 4 and 5 which are near the coast and potentially influenced. Indeed, both stations show typical land-sea breeze-caused diurnal variations in wind speed and direction. Correlation the atmospheric abundances at station 4 with the wind direction reveals high coefficients of r = 0.82 for bromoform, r = 0.73 for dibromomethane and 0.82 for methyl iodide in contrast to the overall negative correlation. According to the position and a mean wind direction of northwest at the 4th station, we get an increase of the trace gas abundances with an increasing easterly component of the wind and a decrease of the abundances with an increasing westerly wind component (not shown). Here, the trace gas variations are related to open ocean and coastal air mass origin as also shown by the trajectories in Fig. 10 in this area. For the 5th station the correlations between wind direction and trace gas abundances only reveals an anti-correlation for the longer lived dibromomethane with r = −0.55. Here, air masses from the open ocean lead to an increase of the dibromomethane abundances, while the variations of bromoform and methyl iodide seem more related to local sources. Three hourly trajectory runs at the 5th station (not shown here) reveal ground-level air masses with potential coastal

ACPD
12, 31205–31245, 2012

and anthropogenic influence along the coast of Western Sahara. Negative correlations of −0.6 to −0.8 are also found between the air pressure and the trace gases. This anti-correlation for the whole cruise is caused by the general weather situation during the ship cruise, especially by predominantly higher pressures at higher latitudes and over open ocean where we observed lower VSLS abundances, and a low pressure system over land southeast of the Mauritanian upwelling (not shown here), coinciding with the increased abundances during station 3–6. At the coastal stations, the anti-correlation is dominated by the atmospheric tides of the air pressure and amounts to −0.5 for bromoform and methyl iodide and even −0.7 for dibromomethane. If this 12 hourly oscillation of sea level pressure related to the trace gas variations can be generalized, has to be investigated in more detail in a future study. Correlating the relative humidity with the trace gases reveals coefficients of 0.5 to 0.6 for open ocean areas and −0.2 to −0.4 at the coastal stations. The vertical distribution of the relative humidity has been a good indicator for mixing in and thickness of the MABL (Sect. 3.1.1), which may point to a co-correlation between the surface relative humidity and the VSLS abundances reflected by the high correlation for the whole cruise. However, over the upwelling areas this relationship does not hold anymore, because evaporation is also, besides the current amount of humidity in the air, depending on the air – and water temperature. Here, ΔT becomes positive, hence we derive a negative sensible heat flux, suppressing convection and leading to a lower relative humidity, which is in contrast to the VSLS abundances. This would explain the reversed correlation above the upwelling. The VSLS abundances are significantly negative correlated with SAT and SST variations in the open ocean and positive correlated with SAT in the coastal upwelling. According to atmosphere–ocean interactions, including heat fluxes from or into the ocean we take the sensible heat flux, in our case reflected by the temperature difference ΔT (T_{SAT}–T_{SST}) into account. We calculate positive correlations of at least 0.7 for all trace gases during the whole cruise and at least 0.6 at the coastal stations. This means, that the combination of higher air – and lower water temperatures coincides with increased trace gas abundances and vice versa, although this is inappropriate for

ACPD
12, 31205–31245, 2012

evaporation and shows that one cannot simply infer from the surface relative humidity on the VSLS abundances or even the MABL height. The temperature difference ΔT further affects the atmospheric stability near the surface. The cold upwelling water at the Mauritanian upwelling converges with warm air from the African coast (Sect. 4.1) and creates a negative sensible heat flux between air and water, which cools the near-surface air layer. As a result surface inversions or at least a stable stratification of the lower atmosphere is formed, which suppresses the vertical movement of air. The resulting reduced volume of air that is available for mixing leads to a low MABL height. An anti-correlation of −0.74 between ΔT and the MABL height at the coastal stations confirms this. A comparison of bromoform, dibromomethane and methyl iodide with the MABL height during the whole cruise is shown in Fig. 11. Higher VSLS concentrations obviously coincide with a lower MABL height and vice versa. During leg 2 the highest mixing ratios are observed while the MABL height stays between the surface and 500 m in the area of the Mauritanian upwelling (stations 3–6). Due to less available air for mixing, the atmospheric mixing ratios of the trace gases increase. On the other hand, the open ocean with low measured mixing ratios coincides with a high boundary layer top. The transit towards Vigo (Spain) also shows a decrease of the MABL height and an increase of the three VSLS mixing ratios close to the Iberian coast. In contrast to the other meteorological parameters we derive throughout negative correlations between the atmospheric trace gas abundances and the MABL height for all regions, reflecting the most distinct connection between these variables. The linear correlations of bromoform, dibromomethane and methyl iodide with the MABL height for the whole cruise are represented in Fig. 12. Bromoform with $r = -0.81$ and dibromomethane with $r = -0.82$ show the highest anti-correlations. Although, the anti-correlation of methyl iodide $r = -0.64$ is not as high as for the brominated halocarbons, probably caused by a difference in its sources, it is significant at the 95 % level.

ACPD
12, 31205–31245, 2012

3.4 Correlations of meteorological parameters with VSLS fluxes

As the sea to air fluxes are calculated depending on wind speed and Δc (Sect. 2.1), we also investigate the influence of other, possibly related meteorological parameters, on the fluxes. As expected, significant positive correlations are observed between wind speed and the VSLS fluxes during the DRIVE campaign (Table 4). The air-sea fluxes are also strongly correlated with Δc between air and sea water (Hepach et al., 2012). Thus the inverse relationship of atmospheric VSLS to MABL height as described in Sect. 3.3 could also have an impact on the regional distribution of their sea to air fluxes: Assuming lower MABL heights and higher atmospheric mixing ratios above the coastal upwelling area, a decrease in the concentration gradient Δc would lead accordingly to lower sea to air fluxes F (Eq. 2). Contrary to this hypothesis, anti-correlations of F to MABL height and an according positive relationship of F to ΔT exists for dibromomethane and bromoform (Table 4). Lower MABL heights with higher atmospheric mixing ratios are found above lower SSTs (Table 3), which were also accompanied by higher production of brominated VSLS in sea water (Hepach et al., 2012). The high oceanic dibromomethane and bromoform concentrations in the coastal upwelling region lead to an increase of Δc and mask the flux suppression by the increasing atmospheric mixing ratios with decreasing MABL height. Methyl iodide in sea surface water showed no distinct regional distribution in contrast to dibromomethane and bromoform (Hepach et al., 2012 to be submitted to ACP). Thus a clear positive correlation of MABL height to its sea to air fluxes would be expected, which is not observed (Table 4). In contrast, the methyl iodide flux reveals only a significant anti-correlation over the upwelling area. Again, the concentration gradient of methyl iodide is strongly driven by its water concentrations leading also neither to a clear positive correlation with MABL height, nor to an inverse relationship with ΔT (not shown here).

Hence we conclude, contrary to the regional distribution of atmospheric VSLS, the regional distribution of their sea to air fluxes is not driven by the MABL height, but by

ACPD
12, 31205–31245, 2012

their sea water concentrations. The impact factors on sea to air fluxes of halogenated VSLS during DRIVE will be further investigated by Hepach et al. (2012).

4 Summary

The diurnal and regional variability of atmospheric VSLS has been investigated during the DRIVE ship campaign in May/June 2010. Additionally, we analyse meteorological influences on the observed VSLS mixing ratios using simultaneous high resolution data. The research area in the eastern tropical and subtropical North Atlantic Ocean around the Canary and Cape Verde Islands, the Mauritanian upwelling and the south-eastern coast of Portugal comprises different oceanic regions, i.e. open ocean and coastal upwelling regions. Six 24 h stations with hourly VSLS measurements were conducted in these areas to contrast regional and diurnal variations. In addition, underway measurements of the VSLS were taken from the coast of Mauritania to Lisbon (Portugal), resulting in a total of 187 atmospheric VSLS measurements during DRIVE. We concentrated our investigation on three trace gases with oceanic sources and different tropospheric lifetimes and ozone depleting potential: bromoform, dibromomethane and methyl iodide. While the mean VSLS mixing ratio over the open ocean for bromoform amounts to 1.74 ppt, for dibromomethane 1.28 ppt and for methyl iodide to 0.93 ppt, increased mean mixing ratios for bromoform of 5.60 ppt, for dibromomethane of 2.37 ppt and for methyl iodide of 1.50 ppt are found above the Mauritanian upwelling. This area also shows diurnal variations of the VSLS with highest fluctuations of 3.57 ppt for bromoform, 0.83 ppt for dibromomethane and 1.85 ppt for methyl iodide. A strong coastal gradient of the VSLS is also observed towards Lisbon (Portugal), where we detect the highest bromoform mixing ratio of the whole cruise of 9.8 ppt.

The air mass origin is investigated by 5-day backward trajectories starting at the surface and at the top of the determined marine atmospheric boundary layer. We identify a predominantly North Atlantic origin of the air due to the prevailing NW winds during the whole cruise with minor coastal influence at the Mauritanian upwelling area.

ACPD
12, 31205–31245, 2012

To distinguish atmospheric constraints on the VSLS we compare several meteorological parameters with the trace gas abundances. Although we do not find an overall relationship with the wind, we detect a significant relation of increasing abundances with easterly wind direction changes (r>0.7) at the 4th station, northwest of Nouakchott (Mauritania), which is linked to land-sea-breeze influence. We also analyse relations with air-sea surface temperature differences. The sensible heat flux, resulting from this difference, influences the near-surface stability of the atmosphere and therefore the marine boundary layer (MABL) height. Thus, temperature difference and MABL height, derived from radiosoundings, are strongly anti-correlated. Variations of the MABL height are depending on the location, as we determine the heights from surface level to reach only up to 400 m in the upwelling region and between 400 to 1700 m over the open ocean. At the Mauritanian upwelling area a so-called stable boundary layer leads to stable atmospheric conditions near the surface, due to warm air flowing over cold upwelling water, suppressing the mixing of air. In the open ocean, the top of the MABL was observed to be limited by trade inversions. Overall a significant anti-correlation between the VSLS mixing ratios and the marine atmospheric boundary layer height is found. With correlation coefficients of $r = -0.81$ for bromoform, $r = -0.82$ for dibromomethane and $r = -0.64$ the MABL has, besides the emitting oceanic sources, a very strong influence on the trace gas mixing ratios. This relationship can explain observed events in the tropical East Atlantic with increased atmospheric VSLS mixing ratios in the upwelling. If this influence can also be found in different seasons or other oceanic regions should be addressed in future studies. Of particular interest would be to investigate other oceanic upwelling regions, which are expected to also have high VSLS sources as the Mauritanian upwelling/Cape Verde Islands region.

ACPD
12, 31205–31245, 2012

The service charges for this open access publication have been covered by a Research Centre of the Helmholtz Association.

Acknowledgements. We thank the authorities of Cape Verde, Mauritania, Portugal and Spain for the permissions to work in their territorial waters. We acknowledge the NOAA Air Resources Laboratory (ARL) for the provision of NCEP Reanalysis data and the HYSPLIT transport and dispersion model used in this publication. We acknowledge the support of the captain and crew of R/V Poseidon as well as Hermann Bange, chief scientist of P399 legs 2 and 3. Financial support of this study was provided by the BMBF grant SOPRAN II FKZ 03F0611A. This work also contributes to the EU project SHIVA (grant no. 226224).

References

Atlas, E., Pollock, W., Greenberg, J., Heidt, L., and Thompson, A.: Alkyl nitrates, nonmethane hydrocarbons, and halocarbon gases over the equatorial Pacific Ocean during SAGA-3, J. Geophys. Res.-Atmos., 98, 16933–16947, doi10.1029/93JD01005, 1993.

Bange, H., Atlas, E., Bahlmann, E., Baker, A., Bracher, A., Cianca, A., Dengler, M., Fuhlbrügge, S., Großmann, K., Hepach, H., Lavrič, J., Löscher, C., Krüger, K., Orlikowska, A., Peeken, I., Quack, B., Schafstall, J., Steinhoff, T., Williams, J., and Wittke, F.: FS Poseidon cruise report P399 legs 2 and 3, IFM-GEOMAR, Kiel, 74, 2011.

Butler, J., King, D., Lobert, J., Montzka, S., Yvon-Lewis, S., Hall, B., Warwick, N., Mondeel, D., Aydin, M., and Elkins, J.: Oceanic distributions and emissions of short-lived halocarbons, Global. Biogeochem. Cy., 21, GB1023, doi:10.1029/2006GB002732, 2007.

Carpenter, L. and Liss, P.: On temperate sources of bromoform and other reactive organic bromine gases, J. Geophys. Res.-Atmos., 105, 20539–20547, doi:10.1029/2000JD900242, 2000.

Carpenter, L., Liss, P., and Penkett, S.: Marine organohalogens in the atmosphere over the Atlantic and Southern Oceans, J. Geophys. Res.-Atmos., 108, GB1023, doi:10.1029/2002JD002769, 2003.

Carpenter, L., Wevill, D., Hopkins, J., Dunk, R., Jones, C., Hornsby, K., and McQuaid, J.: Bromoform in tropical Atlantic air from 25° N to 25° S, Geophys. Res. Lett., 34, L11810, doi:10.1029/2007GL029893, 2007.

ACPD

12, 31205–31245, 2012

Carpenter, L., Fleming, Z., Read, K., Lee, J., Moller, S., Hopkins, J., Purvis, R., Lewis, A., Muller, K., Heinold, B., Herrmann, H., Fomba, K., van Pinxteren, D., Muller, C., Tegen, I., Wiedensohler, A., Muller, T., Niedermeier, N., Achterberg, E., Patey, M., Kozlova, E., Heimann, M., Heard, D., Plane, J., Mahajan, A., Oetjen, H., Ingham, T., Stone, D., Whalley, L., Evans, M., Pilling, M., Leigh, R., Monks, P., Karunaharan, A., Vaughan, S., Arnold, S., Tschritter, J., Pohler, D., Friess, U., Holla, R., Mendes, L., Lopez, H., Faria, B., Manning, A., and Wallace, D.: Seasonal characteristics of tropical marine boundary layer air measured at the Cape Verde Atmospheric Observatory, J. Atmos. Chem., 67, 87–140, doi:10.1007/s10874-011-9206-1, 2010.

Dessens, O., Zeng, G., Warwick, N., and Pyle, J.: Short-lived bromine compounds in the lower stratosphere; impact of climate change on ozone, Atmos. Sci. Lett., 10, 201–206, doi:10.1002/asl.236, 2009.

Garratt, J.: The internal boundary-layer – a review, Bound.-Lay. Meteorol., 50, 171–203, doi:10.1007/BF00120524, 1990.

Gschwend, P., Macfarlane, J., and Newman, K.: Volatile halogenated organic-compounds released to seawater from temperate marine macroalgae, Science, 227, 1033–1035, doi:10.1126/science.227.4690.1033, 1985.

Hepach, H., Quack, B., Wittke, F., Fuhlbrügge, S., Atlas, E. L., Peeken, I., Krüger, K., and Wallace, D. W. R.: Drivers of diel and regional variations of halocarbon emissions from the tropical North East Atlantic, to be submitted to ACP special issu, 2012.

Highwood, E. and Hoskins, B.: The tropical tropopause, Q. J. Roy. Meteor. Soc., 124, 1579–1604, doi:10.1256/smsqj.54910, 1998.

Kalnay, E., Kanamitsu, M., Kistler, R., Collins, W., Deaven, D., Gandin, L., Iredell, M., Saha, S., White, G., Woollen, J., Zhu, Y., Chelliah, M., Ebisuzaki, W., Higgins, W., Janowiak, J., Mo, K., Ropelewski, C., Wang, J., Leetmaa, A., Reynolds, R., Jenne, R., and Joseph, D.: The NCEP/NCAR 40-year reanalysis project, B. Am. Meteorol. Soc., 77, 437-471, doi:10.1175/1520-0477(1996)077< 0437:TNYRP>2.0.CO; 2, 1996.

Kistler, R., Kalnay, E., Collins, W., Saha, S., White, G., Woollen, J., Chelliah, M., Ebisuzaki, W., Kanamitsu, M., Kousky, V., van den Dool, H., Jenne, R., and Fiorino, M.: The NCEP-NCAR 50-year reanalysis: Monthly means CD-ROM and documentation, Bulletin of the American Meteorological Society, 82, 247-267, doi:10.1175/1520-0477(2001)082< 0247:TNNYRM>2.3.CO; 2, 2001.

ACPD
12, 31205–31245, 2012

Kloster, S., Six, K., Feichter, J., Maier-Reimer, E., Roeckner, E., Wetzel, P., Stier, P., and Esch, M.: Response of dimethylsulfide (DMS) in the ocean and atmosphere to global warming, J. Geophys. Res.-Biogeo., 112, G03005, doi:10.1029/2006JG000224, 2007.
Ko, M. K. W., Poulet, G., and Blake, D. R.: Very short-lived halogen and sulfur substances, Scientific assessment of ozone depletion: 2002, Global Ozone Research and Monitoring Project. Report No. 47, Chapter 2, World Meteorological Organization, Geneva, 2003.
Krüger, K. and Quack, B.: Introduction to special issue: The TransBrom Sonne expedition in the tropical West Pacific, ACPD special issue, 12, 1401–1418, 2012.
Manley, S. and Dastoor, M.: Methyl-iodide (CH3I) production by kelp and assoviated microbes, Mar. Biol., 98, 477–482, doi:10.1007/BF00391538, 1988.
Montzka, S. A. and Reimann, S.: Ozone-depleting substances and related chemicals, Scientific Assessment of Ozone Depletion: 2010, Global Ozone Research and Monitoring Project–Report No. 52, Geneva, Switzerland, 2011.
Moore, R. and Tokarczyk, R.: Volatile biogenic halocarbons in the northwest Atlantic, Global. Biogeochem. Cy., 7, 195–210, doi:10.1029/92GB02653, 1993.
Neiburger, M., Johnson, D., and Chien, C.: Studies of the structure of the atmosphere over the Eastern Pacific Ocean in summer: I. The inversion over the Eastern North Pacific Ocean, 1, Univ. of Calif. Publications in Meteorology, 94, 1961.
Nightingale, P., Malin, G., Law, C., Watson, A., Liss, P., Liddicoat, M., Boutin, J., and Upstill-Goddard, R.: In situ evaluation of air-sea gas exchange parameterizations using novel conservative and volatile tracers, Global. Biogeochem. Cy., 14, 373-387, doi:10.1029/1999GB900091, 2000.
O'Brien, L. M., Harris, N. R. P., Robinson, A. D., Gostlow, B., Warwick, N., Yang, X., and Pyle, J. A.: Bromocarbons in the tropical marine boundary layer at the Cape Verde Observatory – measurements and modelling, Atmos. Chem. Phys., 9, 9083–9099, doi:10.5194/acp-9-9083-2009, 2009.
Pyle, J., Warwick, N., Yang, X., Young, P., and Zeng, G.: Climate/chemistry feedbacks and biogenic emissions, Philos T. R. Soc. A, 365, 1727–1740, doi:10.1098/rsta.2007.2041, 2007.
Quack, B. and Wallace, D.: Air-sea flux of bromoform: Controls, rates, and implications, Global. Biogeochem. Cy., 17, 1023, doi:10.1029/2002GB001890, 2003.
Quack, B., Atlas, E., Petrick, G., Stroud, V., Schauffler, S., and Wallace, D.: Oceanic bromoform sources for the tropical atmosphere, Geophys. Res. Lett., 31, L23S05, doi:10.1029/2004GL020597, 2004.

ACPD
12, 31205–31245, 2012

Quack, B., Atlas, E., Petrick, G., and Wallace, D.: Bromoform and dibromomethane above the Mauritanian upwelling: Atmospheric distributions and oceanic emissions, J. Geophys. Res.-Atmos., 112, D09312, doi:10.1029/2006JD007614, 2007.

Raimund, S., Quack, B., Bozec, Y., Vernet, M., Rossi, V., Garcon, V., Morel, Y., and Morin, P.: Sources of short-lived bromocarbons in the Iberian upwelling system, Biogeosciences, 8, 1551–1564, doi:10.5194/bg-8-1551-2011, 2011.

Read, K., Mahajan, A., Carpenter, L., Evans, M., Faria, B., Heard, D., Hopkins, J., Lee, J., Moller, S., Lewis, A., Mendes, L., McQuaid, J., Oetjen, H., Saiz-Lopez, A., Pilling, M., and Plane, J.: Extensive halogen-mediated ozone destruction over the tropical Atlantic Ocean, Nature, 453, 1232–1235, doi:10.1038/nature07035, 2008.

Relvas, P. and Barton, E.: Mesoscale patterns in the Cape Sao Vicente (Iberian Peninsula) upwelling region, J. Geophys. Res.-Oceans, 107, 3164, doi:10.1029/2000JC000456, 2002.

Schauffler, S., Atlas, E., Blake, D., Flocke, F., Lueb, R., Lee-Taylor, J., Stroud, V., and Travnicek, W.: Distributions of brominated organic compounds in the troposphere and lower stratosphere, J. Geophys. Res.-Atmos., 104, 21513–21535, doi:10.1029/1999JD900197, 1999.

Schmittner, A., Oschlies, A., Matthews, H.D, and Galbraith, E.D.: Future changes in climate, ocean circulation, ecosystems, and biogeochemical cycling simulated for a business-as-usual CO emission scenario until year 4000 AD, Global. Biogeochem. Cy., 22, GB1013, doi:10.1029/2007GB002953, 2008.

Seibert, P., Beyrich, F., Gryning, S., Joffre, S., Rasmussen, A., and Tercier, P.: Review and intercomparison of operational methods for the determination of the mixing height, Atmos. Environ., 34, 1001–1027, doi:10.1016/S1352-2310(99)00349-0, 2000.

Skyllingstad, E., Samelson, R., Mahrt, L., and Barbour, P.: A numerical Modeling study of warm offshore flow over cool water, Mon. Weather Rev., 133, 345–361, doi:10.1175/MWR-2845.1, 2005.

Solomon, S., Garcia, R., and Ravishankara, A.: On the role of iodine in ozone depletion, J. Geophys. Res.-Atmos., 99, 20491–20499, doi:10.1029/94JD02028, 1994.

Sorensen, J.: Sensitivity of the DERMA long-range gaussian dispersion model to meteorological input and diffusion parameters, Atmos. Environ., 32, 4195–4206, doi:10.1016/S1352-2310(98)00178-2, 1998.

Stull, R.: An Introduction to Boundary Layer Meteorology, Kluwer Academic Publishers, Dordrecht, 1988.

ACPD
12, 31205–31245, 2012

Sturges, W., Cota, G., and Buckley, P.: Bromoform emission from arctic ice algae, Nature, 358, 660–662, doi:10.1038/358660a0, 1992.
Tegtmeier, S., Krüger, K., Quack, B., Atlas, E. L., Pisso, I., Stohl, A., and Yang, X.: Emission and transport of bromocarbons: from the West Pacific ocean into the stratosphere, Atmos. Chem. Phys., 12, 10633–10648, doi:10.5194/acp-12-10633-2012, 2012.
Troen, I., and Mahrt, L.: A simple-model of the atmospheric boundary-layer: Sensitivity to surface evaporation, Bound.-Lay. Meteorol., 37, 129–148, doi:10.1007/BF00122760, 1986.
Vickers, D., Mahrt, L., Sun, J., and Crawford, T.: Structure of offshore flow, Mon. Weather Rev., 129, 1251–1258, 10.1175/1520-0493(2001)129<1251:SOOF>2.0.CO; 2, 2001.
Vogelezang, D. and Holtslag, A.: Evaluation and model impacts of alternative boundary-layer height formulations, Bound.-Lay. Meteorol., 81, 245–269, doi:10.1007/BF02430331, 1996.
Warwick, N., Pyle, J., Carver, G., Yang, X., Savage, N., O'Connor, F., and Cox, R.: Global modeling of biogenic bromocarbons, J. Geophys. Res.-Atmos., 111, D24305, doi:10.1029/2006JD007264, 2006.
WMO: Definition of the thermal tropopause, WMO Bulletin, 136–137, 1957.
WMO: Scientific Assessment of Ozone Depletion: 2006, Geneva, Switzerland, 572, 2007.
WMO: Scientific Assessment of Ozone Depletion: 2010, World Meteorological Organization, Geneva, 2011.
Yokouchi, Y., Hasebe, F., Fujiwara, M., Takashima, H., Shiotani, M., Nishi, N., Kanaya, Y., Hashimoto, S., Fraser, P., Toom-Sauntry, D., Mukai, H., and Nojiri, Y.: Correlations and emission ratios among bromoform, dibromochloromethane, and dibromomethane in the atmosphere, J. Geophys. Res.-Atmos., 110, D23309, doi:10.1029/2005JD006303, 2005.

ACPD
12, 31205–31245, 2012

Table 1. 24 h stations: position and date.

24 h station	Position	Date/Time
1st	17.6° N, 24.0° W	03.06. (23:00 UTC)–04.06.2010 (22:00 UTC)
2nd	18.0° N, 21.0° W	06.06. (19:00 UTC)–07.06.2010 (17:00 UTC)
3th	18.0° N, 18.0° W	08.06. (18:00 UTC)–09.06.2010 (17:00 UTC)
4th	18.5° N, 16.5° W	10.06. (12:00 UTC)–11.06.2010 (11:00 UTC)
5th	19.0° N, 16.5° W	11.06. (16:00 UTC)–12.06.2010 (15:00 UTC)
6th	20.0° N, 17.25° W	13.06. (04:00 UTC)–14.06.2010 (03:00 UTC)

ACPD
12, 31205–31245, 2012

Table 2. Observed mixing ratios [in ppt] of bromoform ($CHBr_3$), dibromomethane (CH2Br2), their ratio and methyl iodide (CH_3I) for the whole cruise, open ocean (leg 2, except stations 3–6, and leg 3) and coastal stations (stations 3–6). Given are the mean, the range and the standard deviation values.

	$CHBr_3$ (ppt)		CH_2Br_2 (ppt)		CH_3I (ppt)		$\frac{CH_2Br_2}{CHBr_3}$
	mean (range)	stdv of mean	mean (range)	stdv of mean	mean (range)	stdv of mean	mean
whole cruise	3.75 (0.48–9.9)	2.29	1.85 (0.89–3.14)	0.63	1.25 (0.51–3.29)	0.56	0.69
open ocean	1.74 (0.48–9.9)	1.34	1.28 (0.89–2.70)	0.31	0.93 (0.51–2.11)	0.24	0.98
coastal stations	5.60 (4.07–8.92)	1.06	2.37 (1.87–3.14)	0.31	1.55 (0.90–3.29)	0.62	0.43

ACPD
12, 31205–31245, 2012

Table 3. Correlation coefficients of bromoform (CHBr3), dibromomethane (CH2Br2) and methyl iodide (CH3I) with wind speed (wspd), wind direction (wdir), surface air pressure (p), surface air temperature (TSAT), sea surface temperature (TSST), temperature difference ($\Delta T = T_{SAT} - T_{SST}$), relative humidity ($U$), and MABL height for the whole cruise (leg 2 and 3), open ocean (leg 2, except stations 3–6 and leg 3) and coastal stations (stations 3–6). Bold coefficients have a probability of error of less than 5 %.

	$CHBr_3$			CH_2Br_2			CH_3I		
	whole cruise	open ocean	coastal stations	whole cruise	open ocean	coastal stations	whole cruise	open ocean	coastal stations
w_{spd}	0.23	0.23	−0.17	0.27	0.32	−0.05	0.24	0.37	0.06
w_{dir}	−0.49	−0.31	0.04	−0.52	−0.32	−0.18	−0.28	−0.12	−0.01
p	−0.76	−0.01	−0.53	−0.82	−0.11	−0.71	−0.64	−0.33	−0.52
T_{SAT}	−0.04	−0.68	0.42	0.05	−0.67	0.59	0.24	−0.26	0.48
T_{SST}	−0.45	−0.70	−0.04	−0.39	−0.69	0.13	−0.21	−0.24	0.00
ΔT	0.70	0.17	0.64	0.71	0.18	0.63	0.73	−0.13	0.68
U	0.52	0.47	−0.16	0.50	0.58	−0.32	0.21	0.50	−0.38
MABL	−0.81	−0.32	−0.60	−0.82	−0.40	−0.62	−0.64	−0.58	−0.70

ACPD
12, 31205–31245, 2012

Table 4. As Table 3 for fluxes of bromoform, dibromomethane and methyl iodide.

	$CHBr_3$			CH_2Br_2			CH_3I		
	whole cruise	open ocean	coastal stations	whole cruise	open ocean	coastal stations	whole cruise	open ocean	coastal stations
w_{spd}	0.37	0.04	0.48	0.54	0.72	0.70	0.54	0.51	0.60
w_{dir}	−0.37	−0.25	0.05	−0.51	−0.09	−0.13	0.07	0.08	0.09
p	−0.67	−0.27	−0.58	−0.81	−0.73	−0.73	−0.08	−0.17	−0.12
T_{SAT}	−0.08	−0.40	0.15	−0.06	−0.79	0.27	−0.20	−0.22	−0.23
T_{SST}	−0.54	−0.52	−0.31	−0.51	−0.86	−0.16	−0.24	−0.30	−0.35
ΔT	0.76	0.22	0.68	0.75	−0.11	0.62	0.12	0.16	0.19
U	−0.04	0.18	−0.44	−0.02	0.69	−0.60	−0.08	0.12	−0.25
MABL	−0.58	−0.29	−0.61	−0.68	−0.94	−0.70	−0.27	0.26	−0.55

ACPD
12, 31205–31245, 2012

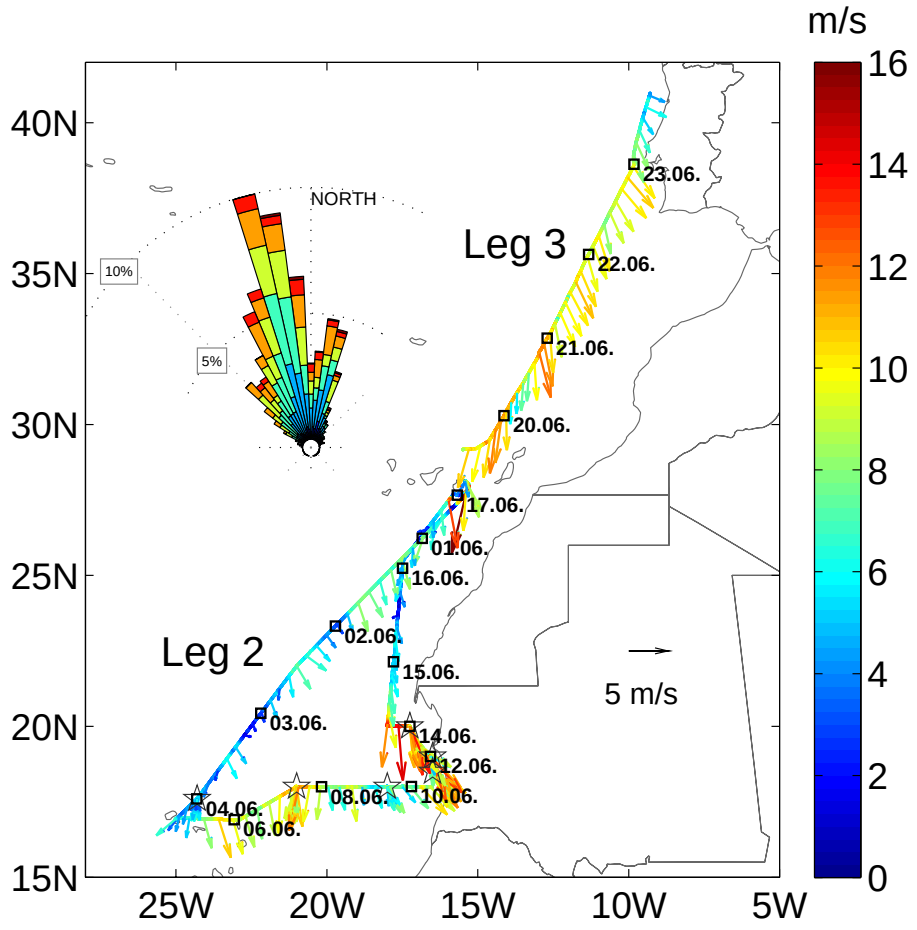

Fig. 1. DRIVE cruise track. In addition the 3 hourly wind speed [m s^{-1}] and direction (10 min averages) and windrose for the whole cruise are shown.

ACPD
12, 31205–31245, 2012

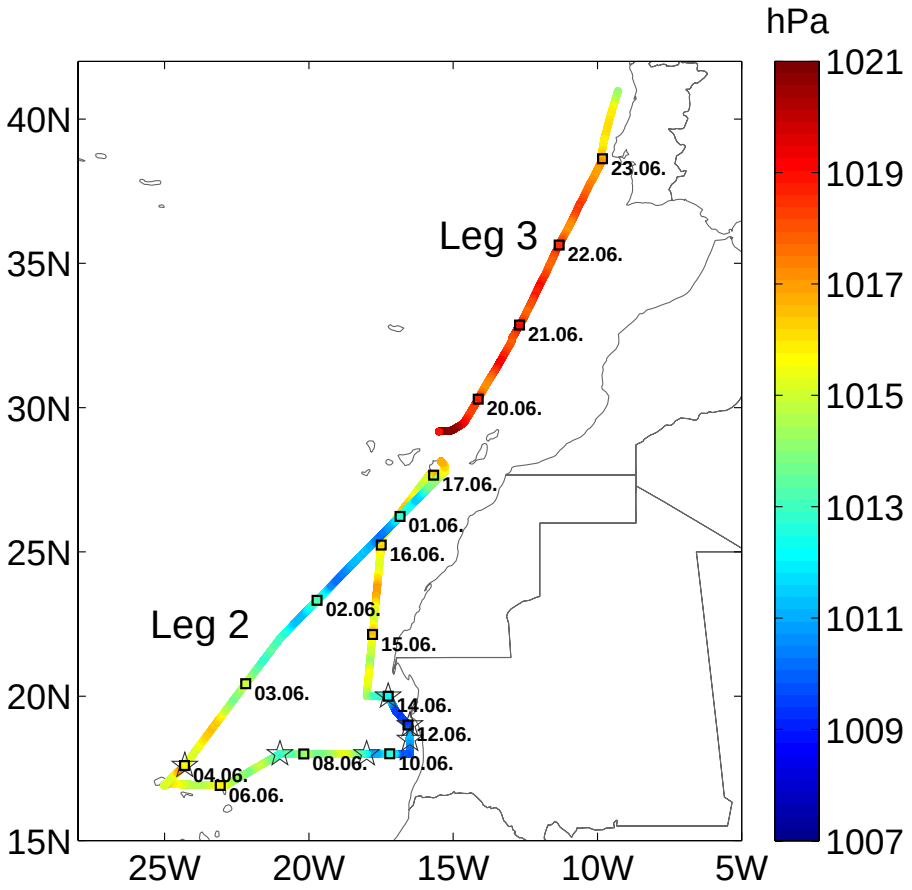

Fig. 2. 10 min average measurements of air pressure [hPa]. The stars indicate position and time of the diurnal stations.

ACPD
12, 31205–31245, 2012

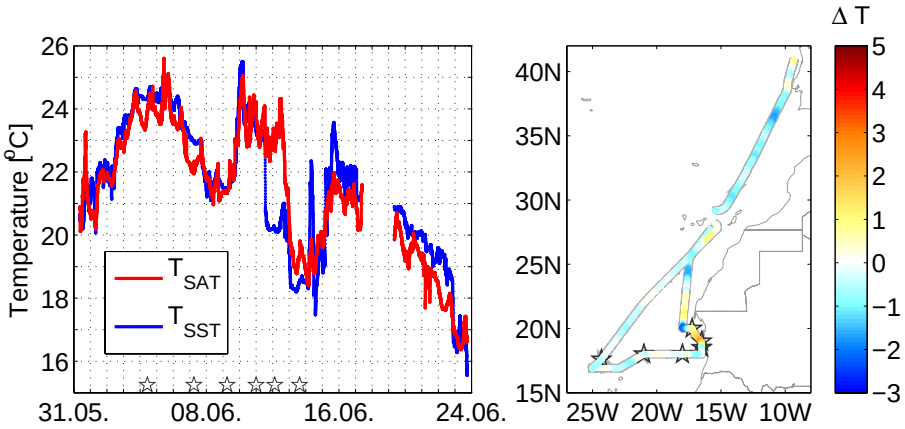

Fig. 3. Left: 10 min average measurements of TSAT and TSST [°C]. The stars indicate position and time of the diurnal stations. Right: the temperature gradient is given in [K].

ACPD
12, 31205–31245, 2012

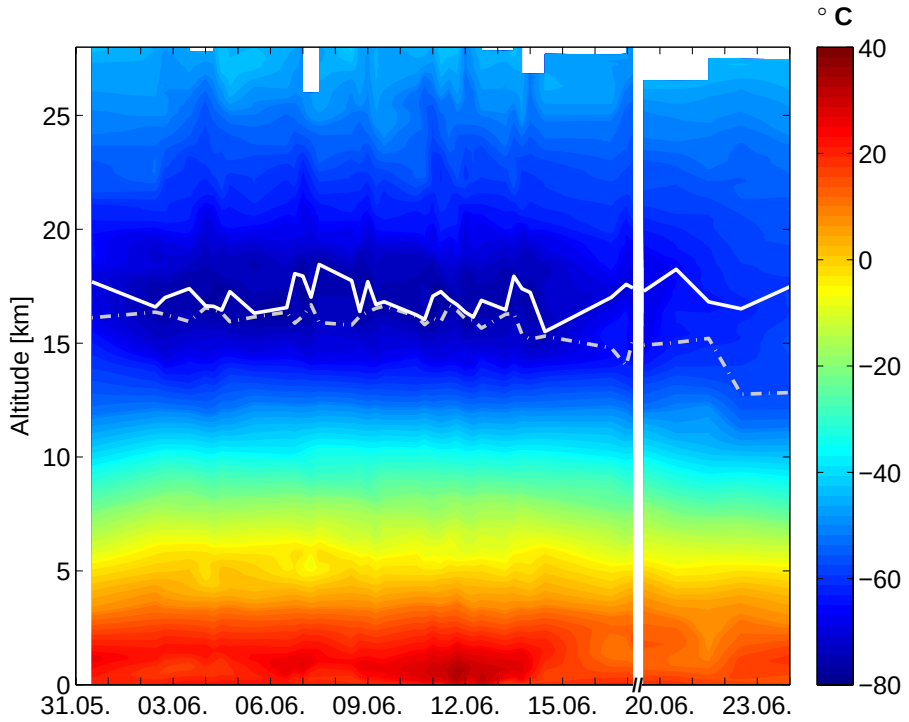

Fig. 4. Air temperature cross sections [°C] from radiosoundings for the whole cruise. Cold point tropopause and lapse rate tropopause are marked by the continuous and the dash-dotted lines, respectively. The measurement gap between leg 2 and 3 is shortened.

ACPD
12, 31205–31245, 2012

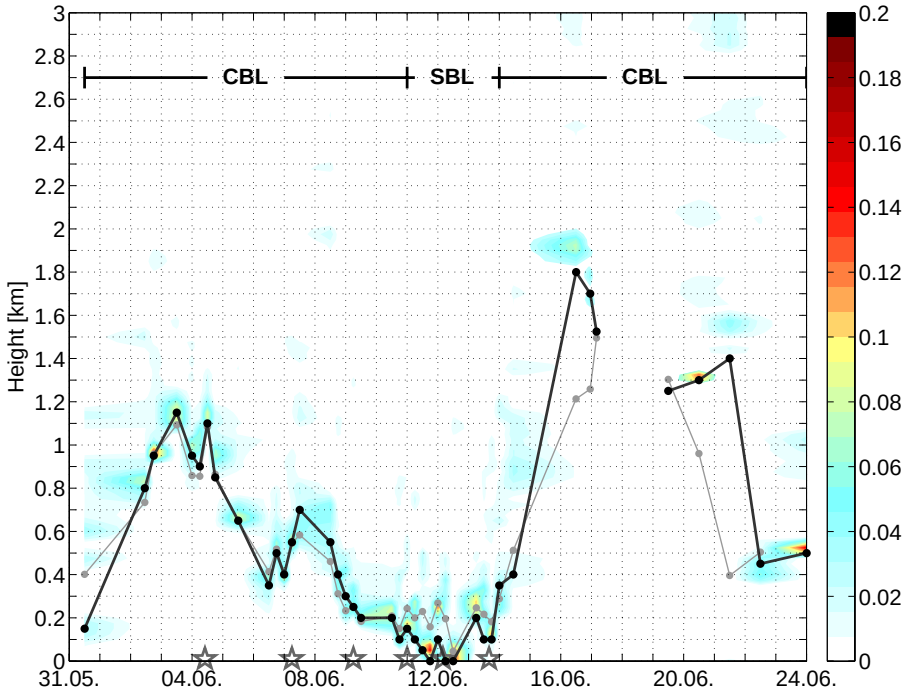

Fig. 5. Virtual potential temperature gradient (colour shading, in K) with derived MABL heights (lines, in km). The black line shows the subjectively determined MABL height from temperature and humidity profiles and the grey line is determined theoretically (Sect. 2). CBL and SBL identify convective and stable boundary layers. The 24 h stations are markedwith stars.

ACPD
12, 31205–31245, 2012

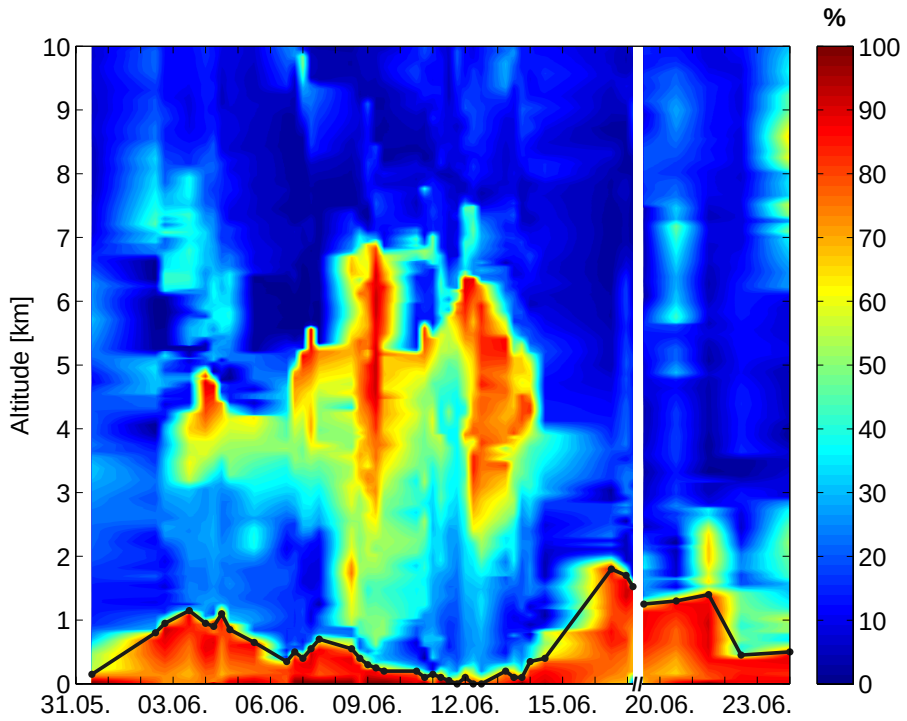

Fig. 6. Relative humidity cross sections [%] from radiosoundings for the whole cruise. The subjectively determined MABL height [km] is marked by the black line. The measurement gap between leg 2 and 3 is shortened.

ACPD
12, 31205–31245, 2012

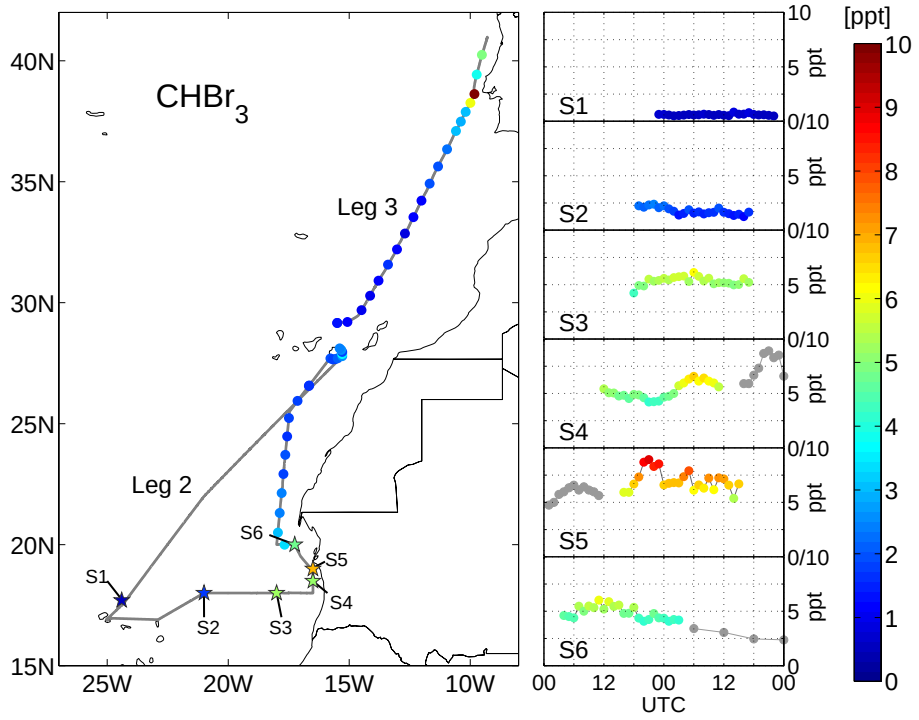

Fig. 7. Bromoform mixing ratios [ppt] measured during the DRIVE ship campaign from 31 May to 24 June 2010. Six 24 h stations (S1–S6) and underway measurements are color-coded according to the scale on the right side.

ACPD
12, 31205–31245, 2012

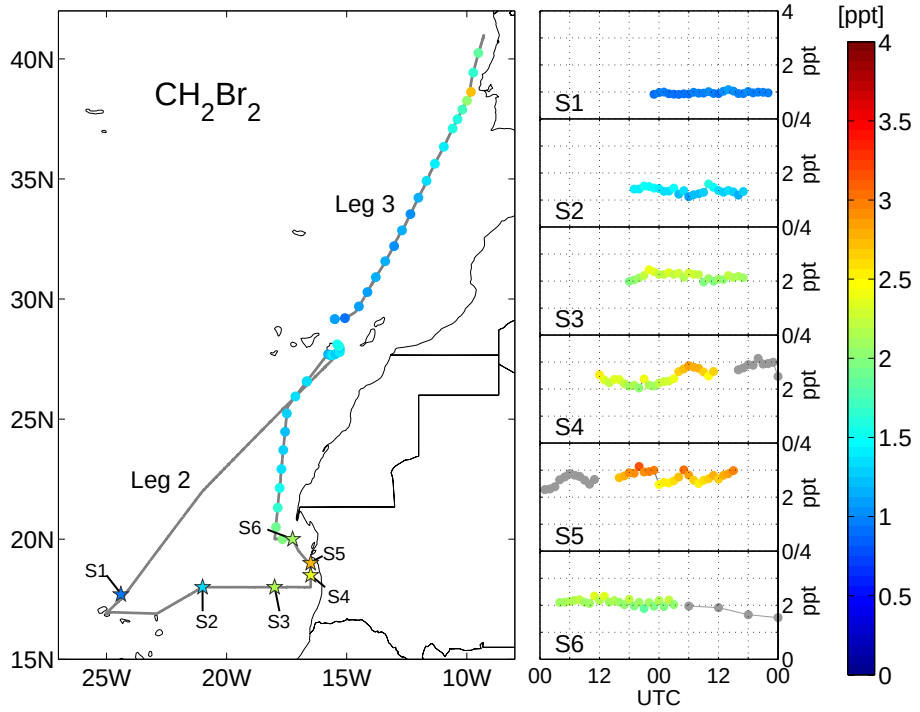

Fig. 8. As Fig. 7 for dibromomethane.

ACPD
12, 31205–31245, 2012

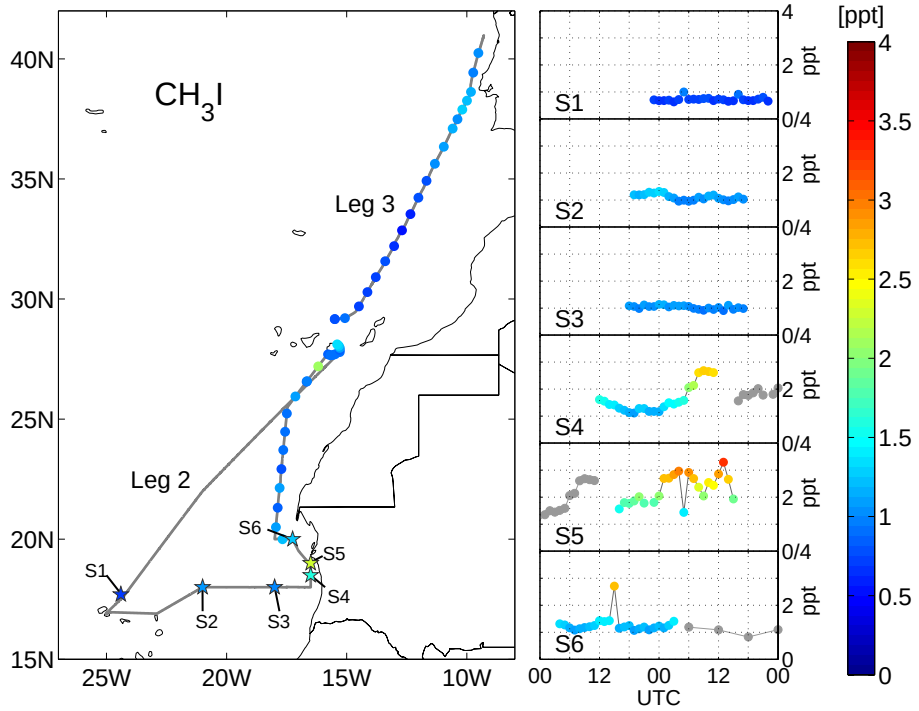

Fig. 9. As Fig. 7 for methyl iodide.

ACPD
12, 31205–31245, 2012

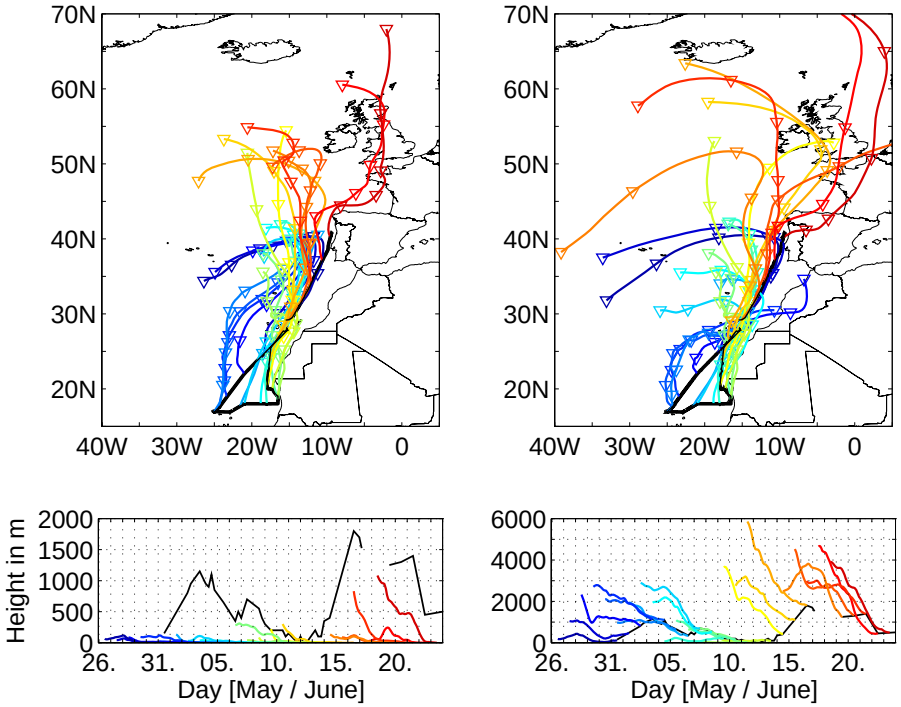

Fig. 10. HySplit 5-day backward trajectories: initiated at the surface (left side) and at the top of the determined marine atmospheric boundary layer (right side). The lower panels show the vertical extension of the backward trajectories, the black line indicates the height of the MABL; both are given in [m].

ACPD
12, 31205–31245, 2012

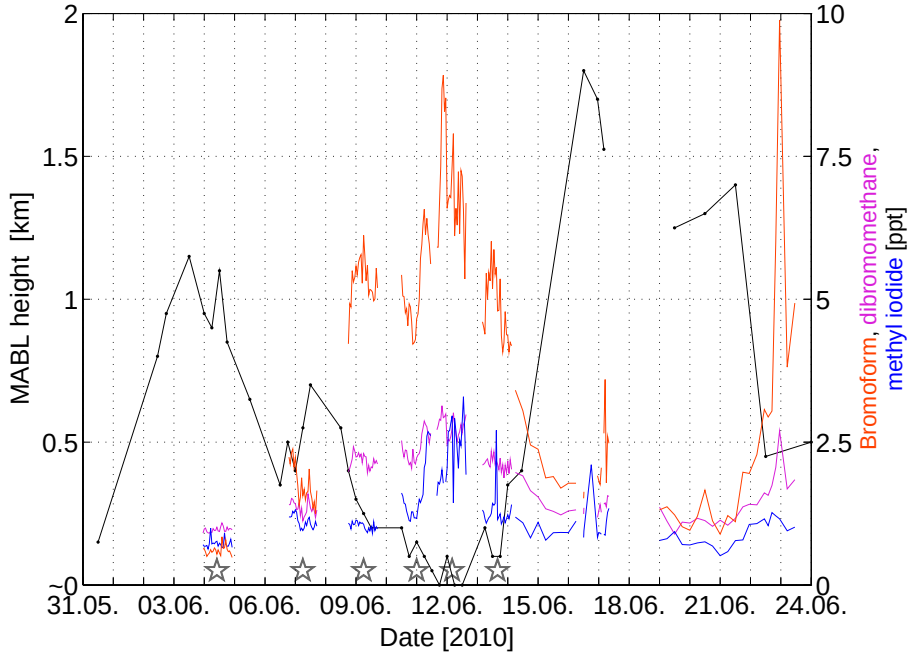

Fig. 11. Comparison of MABL height (left scale, in km) with bromoform, dibromomethane and methyl iodide (right scale, in ppt).

ACPD
12, 31205–31245, 2012

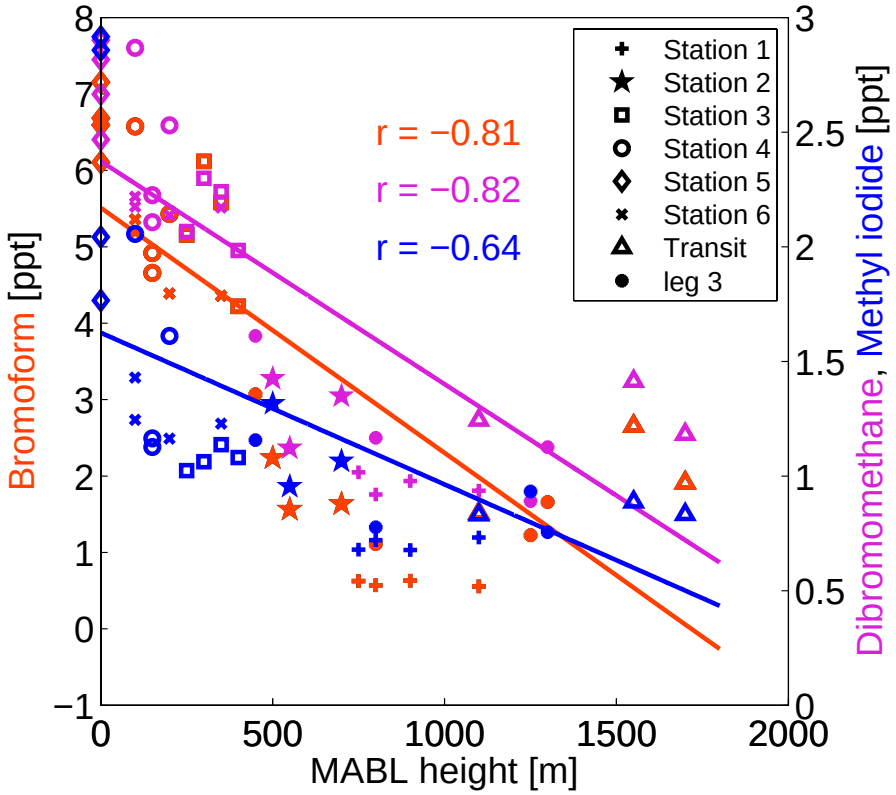

Fig. 12. Correlation between VSLS abundances [ppt] and MABL height [m] for the whole cruise.

ACPD
12, 31205–31245, 2012